SCIENTIFIC REPORTS

OPEN

Multiomics analysis of the giant triton snail salivary gland, a crown-of-thorns starfish predator

Received: 23 January 2017
Accepted: 2 June 2017
Published online: 20 July 2017

U. Bose[1,2], T. Wang[1], M. Zhao[1], C. A. Motti[2], M. R. Hall[2] & S. F. Cummins[1]

The giant triton snail (*Charonia tritonis*) is one of the few natural predators of the adult Crown-of-Thorns starfish (COTS), a corallivore that has been damaging to many reefs in the Indo-Pacific. *Charonia* species have large salivary glands (SGs) that are suspected to produce either a venom and/or sulphuric acid which can immobilize their prey and neutralize the intrinsic toxic properties of COTS. To date, there is little information on the types of toxins produced by tritons. In this paper, the predatory behaviour of the *C. tritonis* is described. Then, the *C. tritonis* SG, which itself is made up of an anterior lobe (AL) and posterior lobe (PL), was analyzed using an integrated transcriptomics and proteomics approach, to identify putative toxin- and feeding-related proteins. A *de novo* transcriptome database and *in silico* protein analysis predicts that ~3800 proteins have features consistent with being secreted. A gland-specific proteomics analysis confirmed the presence of numerous SG-AL and SG-PL proteins, including those with similarity to cysteine-rich venom proteins. Sulfuric acid biosynthesis enzymes were identified, specific to the SG-PL. Our analysis of the *C. tritonis* SG (AL and PL) has provided a deeper insight into the biomolecular toolkit used for predation and feeding by *C. tritonis*.

If a generalist predator evolves to a more a specialist diet, it is assumed that it would be accompanied by modifications of characters that permit greater efficiency in capturing specific prey species. These likely include foraging behaviors and search strategies with fine-tuned chemosensory systems, physiological processes associated with digestion and waste removal, and other features involved with prey capture[1]. Among predatory taxa the evolution of a specialized diet is likely to be strongly linked to the evolution of venoms used to subdue prey. Although the evolution of many of these characters may be difficult to trace for a species that has evolved a restricted diet, the evolution of venoms can be inferred from analyses of expression of genes encoding venom and digestion components[2,3].

Marine organisms from a broad range of phyla, from bacteria and algae to invertebrates and vertebrates, are known to produce toxins with high chemical diversity, divergence of which is likely driven by speciation and diet[4–6]. Some examples include tetrodotoxins produced by bacteria found in the saliva of the blue-ringed octopus and puffer fish[7,8], potent pore-forming toxins produced by cnidarians[9], okadaic acid produced by bacteria in marine sponges[10], and saponins (steroidal and triterpenoid) that are produced by echinoderms[11]. Venoms, and in particular specific toxins, play multiple roles from foraging to defense and intraspecific conflict[12]. Although there are many species of predatory marine snails, studies of venom toxins have been restricted to species within the superfamily Conoidea[13]. These venomous marine cone snails synthesize a remarkable diversity of pharmacologically active small peptides (conotoxins) to enable prey capture, self-defense and intra-specific competition[14–16]. The potency and selective profiles of the conotoxins vary depending on species targets that may include various subtypes of voltage- and ligand-gated ion channels, G protein-coupled receptors and neurotransmitter transporters[17].

Gastropods of the superfamily Tonnoidea are effective predators and thought to capture prey through envenomation[18]. Within the Tonnoidea, several species in the Cassidae family of snails are specialist predators of echinoderms. The large paired and mono-lobed salivary gland (SG) of Cassidae family snails are known to be toxic and inject a strong acid or venomous saliva into their prey to paralyse them before consumption[19–21]. For example, Cassidae helmet shell snails secrete an acidic saliva to soften the body wall of their preferred prey, sea urchin[22,23],

[1]Faculty of Science, Health, Education and Engineering, Genecology Research Center, University of the Sunshine Coast, Maroochydore DC, Queensland, 4558, Australia. [2]Australian Institute of Marine Science, Townsville, Queensland, 4810, Australia. Correspondence and requests for materials should be addressed to S.F.C. (email: scummins@usc.edu.au)

through which they bore a wide hole using their radula apparatus and long proboscis[22]. In *Cassidaria echinophora* and *Tonna galea* sulfuric acid is secreted through their proboscis[24,25]. The saliva of *Cassis tuberosa* can immobilize the spines of sea urchin[18]. Within the Tonnidae group of marine snails, which also predate crustaceans and bivalve molluscs, large SGs have been identified that produce complex salivary secretions[26].

The giant triton snail *Charonia tritonis* (superfamily Tonnoidea) is found on reefs throughout the Indo-Pacific where it predates upon echinoderms including starfish, sea cucumbers and sea urchins[27–29]. Giant tritons rely on their highly developed olfactory sense to track and locate prey[30,31]. Upon contact with prey, they initiate a 'tapping' behaviour using their cephalic tentacles. Although the prey attempts to escape, the giant triton immobilizes it initially by mechanical means, positioning its large muscular foot over the aboral surface. This is rapidly followed by insertion of the proboscis and most likely injection of venom(s) that paralyses the prey[27,30]. At least several species within the Ranellidae (Tonnidea) are known to produce sulphuric acid to access their prey[32]. The marine gastropoda, *Gyrineum natator* uses sulfuric acid to capture their bivalve prey and also use this acid for their defense[32]. The turban shell, *Lunella coronate* possesses sulphuric acid-producing glands which are used for their defense, to externally digest its accessed prey or to attack less accessible prey[33]. It has been proposed that the Atlantic triton snail (*Charonia variegate*) possesses toxins derived from its foot or mouth which may assist to immobilize prey[34]. In the knobbed triton snail (*Charonia lampas rubicunda*), the proboscis delivers a SG secretion that induces instant paralysis of the sea star *Patriella brevispina*[35]. Recently a peptide venom was identified within the SG of the hairy triton snail, *Monoplex parthenopeus* (Subfamily Cymatiinae)[36,37]. Conversely, another study on *C. lampas* feeding behavior found no evidence of the injection of either venom or acid[30], although it should be noted that to date, SGs of *C. lampas* have not been analysed for the presence of such biomolecules[30].

Based on feeding trials with *C. tritonis*, their preferred prey includes the crown-of-thorns starfish (COTS), *Acanthaster planci*, a corallivore asteroid that has contributed to mass coral loss throughout Indo-Pacific coral reefs[35]. However, *C. tritonis* are either naturally rare or endangered due to unregulated harvesting, with many countries now prohibiting their collection. Whatever the case, it has been proposed that the giant triton, as a major predator of COTS, has a role sin regulating the populations of COTS. For this reason, it is desirable to assess basic processes of their biology to assist in the potential development of captive breeding programs for release of giant tritons onto reefs infested with COTS. Consumption of COTS would require a special digestive strategy especially as COTS not only present a formidable physical defense in the form of sharp aboral spines but also contain and secrete various sulfated steroidal saponins and toxins[38]. Saponins are toxic and can deter their predators. Therefore, it is likely that giant triton snails have evolved specific traits to combat their effects[35]. Although an early study by Endean (1972) indicated that *Charonia* sp. uses venom to paralyze their prey, questions remain as to the chemical nature of these, and what role they play in the capture, immobilization and digestion of COTS[35].

In this study, we describe the behaviour associated with *C. tritonis* COTS predation. Following an anatomical analysis of the *C. tritonis* SG, we have performed next-generation transcriptome sequencing and annotation of ensuing transcripts in association with proteomic analyses. We report for the first time the existence of numerous secreted proteins, including a diverse array of putative toxin- and feeding-like protein families in *C. tritonis*.

Materials and Methods

Triton behaviour in response to COTS. *C. tritonis* (N = 8) were collected from the Great Barrier Reef under special permit (G13/36390.1) and held in a 4,000 L indoor 4 m^2 diameter holding tank at ambient temperature (26–28 °C) and salinity (32–35 ppt) with simulated natural photoperiod at the Australian Institute of Marine Science (AIMS). Water current in the tank (clockwise) was induced through airlifts via three 5 cm diameter PVC pipes with water intake at the base of the tank and expulsion through a 90 degree elbow at the surface. The giant tritons were periodically presented with live COTS, between 1 to 2 COTS per giant triton per week. General observations were made on the reaction of the giant tritons as well as the COTS and video recorded on GoPro over 8 h.

Anatomy and tissue collection. For tissue collection, wild *C. tritonis* were collected from Kavieng, Papua New Guinea and temporarily held and fed on echinoderms at the Marine Research Station, Kavieng. Animals were anaesthetized with isotonic $MgCl_2$ and the anterior portion removed from the shell. During the dissection the proboscis and SG were photographed using an iPhone 6 (8 MP, phase detection autofocus, dual-LED, Apple Inc. USA). For analysis of SG cell composition, the gland was spread onto a slide, then viewed and photographed using a Leica microscope equipped with a CCD camera. SGs were dissected and separated into the anterior lobe (AL) and posterior lobe (PL). Tissues collected for RNA isolation were stored in RNAlater (Ambion, California). For protein isolation, tissues were processed immediately as described below.

RNA isolation, sequencing and transcriptome assembly. RNA was extracted from tissue using TRIzol Reagent (Invitrogen Corp., Carlsbad, CA, USA), as per the manufacturers protocol. Following extraction, RNA was assessed for quality by visualisation on a 1.2% agarose gel, and quantified using a Nanodrop spectrophotometer (Thermo scientific). Total RNA samples were sent to Australian Genome Research Facility (Brisbane, Australia) for library construction and sequenced (paired-end) using an Illumina HiSeq 2500 sequencing platform. Raw sequence reads (100 bp) were assembled into contigs (>200 bp) using the CLC genomics software (Qiagen). Protein coding regions were determined using the open reading frame (ORF) predictor[39]. Relative expression of genes in each tissue transcriptome was determined based on RPKM (Reads Per Kilobase of exon per Million mapped reads) values, utilizing the commercially available CLC Genomic Workbench 7 software[40].

Gene annotation, protein models and prediction of secreted proteins (exoproteome). A BLASTp search was used to annotate proteins from each *C. tritonis* transcriptome. Schematic diagrams of protein domain structures were prepared using IBS illustrator (IBS, version 1.0) software[41]. Multiple sequence

alignments were performed using the MEGA 6.0 platform with the ClustalW protocol and the Gonnet protein weight matrix[42]. SWISS-MODEL[43] was used to predict the 3D protein structure of an echotoxin-like protein identified from giant triton SG[44]. First, BLASTp analysis was used to identify a template that shared significant sequence similarity to a *C. tritonis* echotoxin sequence. The best match was selected based on the presence of similar domains and plausibility quality control. Finally, based on the alignment, the coordinates of the model were constructed for the structurally conserved regions of the model. N-terminal signal sequences were predicted using the SignalP 4.1[45], Predisi[46] and TMHMM[47]. A protein was designated as secreted only when it met the criteria of both SignalP and Predisi, and did not have a transmembrane domain predicted by TMHMM. Simple Modular Architecture Research Tool (SMART) was used to identify conserved domains in SG proteins[48]. Glycosylation sites were identified by using NetNGlyc 1.0 server[49].

Protein isolation from salivary gland lobes and nanoHPLC-ESI-Triple TOF. Frozen samples of SG lobes were homogenized in protein extraction buffer (8 M urea, 4 M thiourea, 0.8 M NH_4HCO_3, pH 8.0) in a 1:5 w:v ratio. Crude extracts were then centrifuged for 20 min (12,000 xg, 4 °C), then supernatant was collected, fractionated by 1D SDS-PAGE and stained using Coomassie Blue (GE Healthcare, city). Gel bands were excised and digested with trypsin following the protocol described previously[50]. Before LC-MS analysis, Zip-tip C18 (Merck Millipore, USA) was used to desalt and concentrate peptides and small proteins.

Tryptic peptides were further analysed by liquid chromatography-tandem mass spectrometry (LC-MS/MS) on a Shimadzu Prominance Nano HPLC (Japan) coupled to a Triple-TOF 5600 mass spectrometer (ABSCIEX, Canada) equipped with a nano electrospray ion source. Aliquots (6 µL) of each extract were injected onto a 50 mm × 300 µm C18 trap column (Agilent Technologies, Australia) at 30 µL/min. The samples were desalted on the trap column for 5 min using solvent A [0.1% formic acid (aq)] at 30 µL/min. The trap column was then placed in-line with a 150 mm × 75 µm 300SBC18 3.5 µm analytical nano HPLC column (Agilent Technologies) for mass spectrometry analysis. Peptides were eluted with a linear gradient of 1–40% solvent B [90:10 acetonitrile: 0.1% formic acid (aq)] over 35 min at 300 nL/min flow rate, followed by a steeper gradient from 40% to 80% solvent B over 5 min. Solvent B was then held at 80% for 5 min to wash the column and then returned to 1% solvent B for equilibration before the next sample injection. The ionspray voltage was set to 2400 V, declustering potential (DP) 100 V, curtain gas flow 25, nebuliser gas 1 (GS1) 12 and interface heater at 150 °C. The mass spectrometer acquired 500 ms full scan TOF-MS data followed full scan (20 × 50 ms) product ion data in an Information Dependent Acquisition (IDA) mode. Full scan TOF-MS data was acquired over the mass range 350–1800 m/z and for product ion MS/MS 100–1800 m/z. Ions observed in the TOF-MS scan exceeding a threshold of 100 counts and a charge state of +2 to +5 were set to trigger the acquisition of product ion, MS/MS spectra of the resultant 20 most intense ions. The data was acquired and processed using Analyst TF 1.5.1 software (ABSCIEX, Canada).

Proteins were identified by database searching using PEAKS v7.0 (BSI, Canada) against the protein database built from the *C. tritonis* SG lobe transcriptomes. Search parameters were as follows: precursor ion mass tolerance, 0.1 Da; fragment ion mass tolerance, 0.1 Da; fully tryptic enzyme specificity with two possible missed cleavage sites; monoisotopic precursor mass; a fixed modification of cysteine carbamidomethylation; and variable modifications which included methionine oxidation, conversion of glutamine and glutamic acid to pyroglutamic acid, acetylation of lysine and deamidation of asparagine; false discovery rate (FDR) was set to $\leq 1\%$, and (-10*lgP) was calculated accordingly where P is the probability that an observed match is a random event.

Results and Discussion

***C. tritonis* hunting behavior.** Aquatic invertebrates primarily rely on their olfactory sense to detect and locate potential prey[51]. The otherwise mainly sedentary COTS exhibited extreme agitation and movement when placed into the tank holding giant tritons. Similarly, sedentary giant tritons become active within a few minutes of exposure to the scent of COTS exhibiting a sweeping motion of both tentacles and forward movement. In a 4 m diameter tank with a clockwise water flow tritons would track the odour of COTS by moving counter-clockwise into the current even if the prey item was within 0.5 m of it down current. The COTS themselves are known to detect the odour of giant tritons and, rather than being normally sedentary, would exhibit pronounced movement[31]. A previous study had observed that *C. tritonis* hunting behavior (upon various echinoderm species, including COTS) was most prominent in the evening (57.1%), compared to morning (35.7%) and afternoon (7.1%)[52]. We observed that the entire hunt, attack and consumption of COTS could be completed within 4 h.

Tritons were documented hunting, attacking and feeding on COTS (Supplementary Video S1). Upon initial contact with COTS, the snails' large muscular foot covers the COTS arms to suppress movement. Simultaneously, *C. tritonis* retract then elongated their proboscis and moves it gradually around the base of the spines until insertion into the central disc area (Fig. 1A–C). It is possible that the proboscis seeks to cut the circumoral neural ring, as the COTS, while highly alarmed at this stage, become uncoordinated with no directional movement. At this point, the *C. tritonis* begin to saw into the COTS flesh using their radula. Closer inspection of the internal anatomy of the *C. tritonis* proboscis reveals the muscle, ducts, and buccal mass housing the radula at the proboscis tip (Fig. 1D). The radulae have been described in significant detail for other triton species, through scanning electron microscopy, showing the presence of cuspless marginal teeth and variations within the shape of central teeth[36]. Giant triton snails produce a prolific amount of mucus during the attack and consumption of the COTS, which may be associated with sequestration and possibly detoxification of saponins released by COTS or to absorb saponins before they reach the interior of the shell and make contact with the gills. Saponins readily cross the gills of fish and lyse red blood cells causing respiratory distress and in high enough concentration can cause death[53]. The terrestrial slug, *Arion lusitanicus*, has been shown to sequester and detoxify alkaloids from a variety of plants[54]. Given that giant tritons are not only exposed to secreted saponins during the attack but also ingest them in high concentrations, it is likely that they can metabolise saponins. Metabolic pathways for saponin

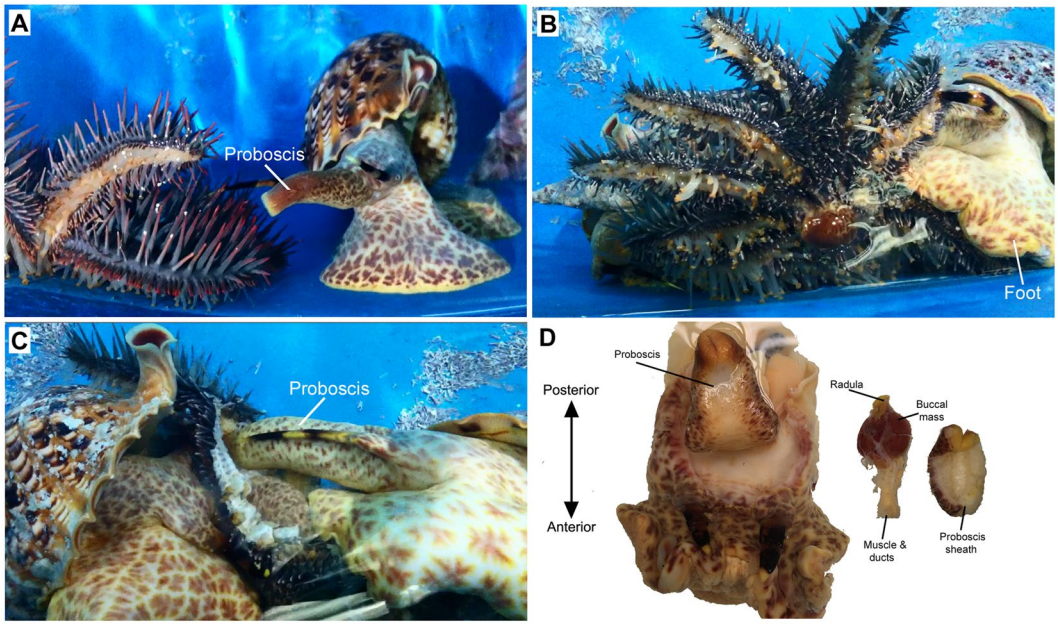

Figure 1. *Charonia tritonis* attack on a Crown-of-Thorns starfish (COTS). (**A**) *C. tritonis* withdraws proboscis in preparation for attack. (**B**) *C. tritonis* uses muscular foot to immobilize COTS. (**C**) Two *C. tritonis* feeding on a COTS, proboscis of the snail on the right penetrating COTS body wall. (**D**) Location of the proboscis, and internal organs including buccal mass, ducts and radula in *C. tritonis*.

detoxification mechanisms have been described for plant-fungi interactions, where the fungi contains genes that encode enzymes that break down plant saponins, leading to disease resistance[55,56].

***C. tritonis* salivary gland anatomy and transcriptome assembly.** In those Tonnoidea investigated to date, SGs are paired, with each gland divided into two parts: the smaller tubular or acinous anterior lobes (AL) and the voluminous posterior lobes (PL) that putatively secrete sulphuric acid[19,24,25,36]. Their size, shape and structure may vary significantly between genera and those species within[36]. The *C. tritonis* paired SGs were identified within the region of the foregut, similarly split morphologically into anterior and posterior lobes; the AL is larger and has an orange appearance, while the PL is smaller and white (Fig. 2A–D). This is in contrast to what is observed in other Tonnoidea, where the PL is the larger lobe. The histology of the SG has been described for two Tonnoidea, the *Argobuccinum pusulosum* and *Monoplex intermedius*, showing a posterior salivary duct entering the inside of the anterior lobe[21,57]. In this study, no histology was performed, however, a cell smear of the AL revealed a mixture of cells, with large and clear cells supported by mucin-like molecules being the most prominent (Fig. 2E). In *C. intermedius*, the fine structure analysis of the salivary glands has revealed posterior acid secreting and acinous anterior lobes[21]. Transverse sections through the posterior SG of the *C. lampas* show many cells that appear to contain a basophilic mucus[30].

Raw sequence RNA-seq reads were obtained for both AL and PL of the *C. tritonis* SG using Illumina technologies (NCBI PRJNA383875), then assembled into transcriptome library contigs. In the SG-AL, there were 84,807,390 total filtered reads assembled into 105,955 contigs, 105,297 ORFs (Supplementary Data S1) and 18,729 ORFs that have a BLASTp match to a known protein (Supplementary Data S2a). Likewise, in the SG-PL there were 81,597,308 total filtered reads assembled into 115,171 contigs, 114,289 ORFs (Supplementary Data S3) and 19,005 ORFs that have a BLASTp match to a known protein (Supplementary Data S4a).

In silico exoproteome prediction and proteomic analysis. An *in silico* analysis was performed to identify putative SG secreted proteins, which predicted that the SG-AL and SG-PL secrete 3,805 and 3,860 proteins, respectively; all contain signal peptides and no transmembrane domains (Supplementary Data S2b and S4b). Due to technical limitations, proteins were extracted from crude intact SG-AL and SG-PL, rather than performing gland 'milking' which is now recognized as a more efficient method for obtaining cone snail venom[58]. Crude protein extracts were initially separated by SDS-PAGE and viewed by Coomassie staining, demonstrating the presence of a large number of proteins with a high-low molecular weight distribution (Fig. 3A). Bands that were extracted from fractionated SG-AL revealed 191 proteins (Supplementary Data S3c). Further annotation (BLASTp, signal peptide, transmembrane domain) indicated that 27 of these proteins have BLAST matches and features typical of secreted proteins. (Supplementary Data S2d and Supplementary Data S5). All of these proteins have a homolog within the *C. reticulate* salivary transcriptome. Fractionated SG-PL extracts revealed 775 proteins (Supplementary Data S4c), including 59 proteins that have features consistent with being secreted (Supplementary Data S4d and Supplementary Data S6). Four of these proteins do not have any homology with any derived protein within the *C. reticulate* salivary transcriptome. All total proteins identified could be placed into Pfam categories (protein

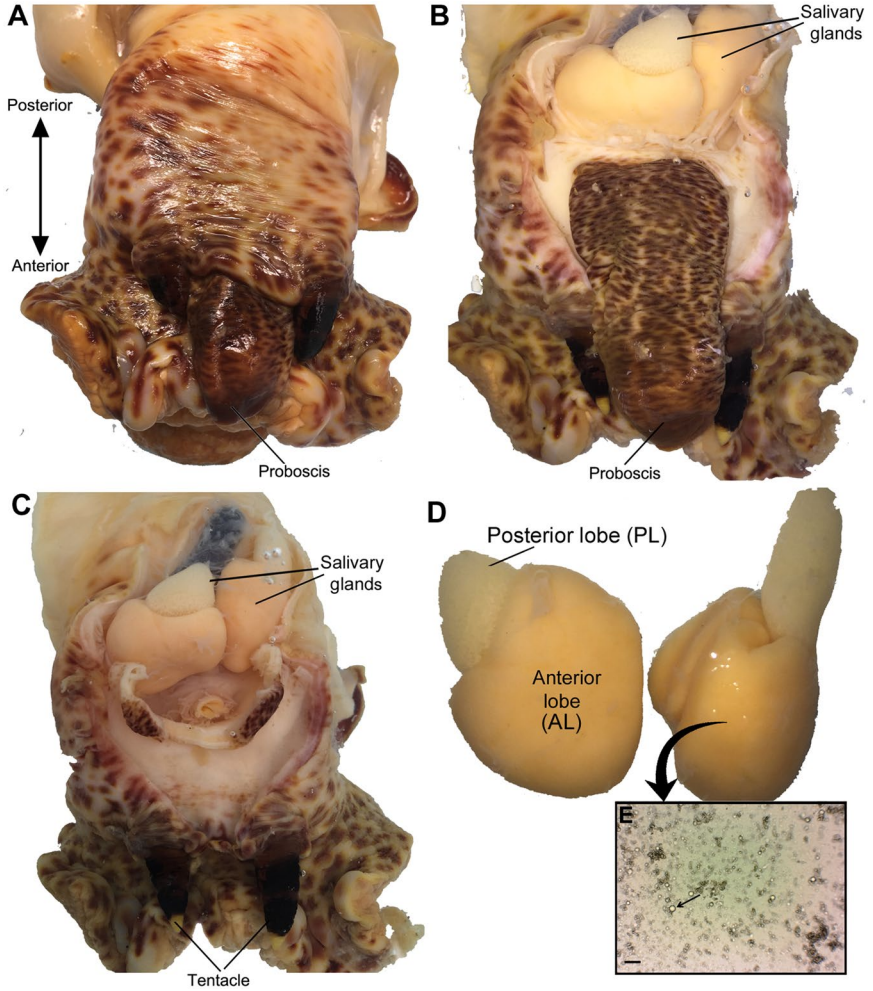

Figure 2. *Charonia tritonis* salivary gland (SG) anatomy and proteomics study. (**A**) Cephalic region of the *C. tritonis*. (**B**) Cephalic region with full proboscis and paired SGs exposed. (**C**) Cephalic region with proboscis removed. (**D**) Isolated SG showing region of anterior lobe (AL) and posterior lobe (PL). (**E**) Cell smear of AL. Arrow shows prominent mucin-like globlet cell. Scale bar represents 200 μm.

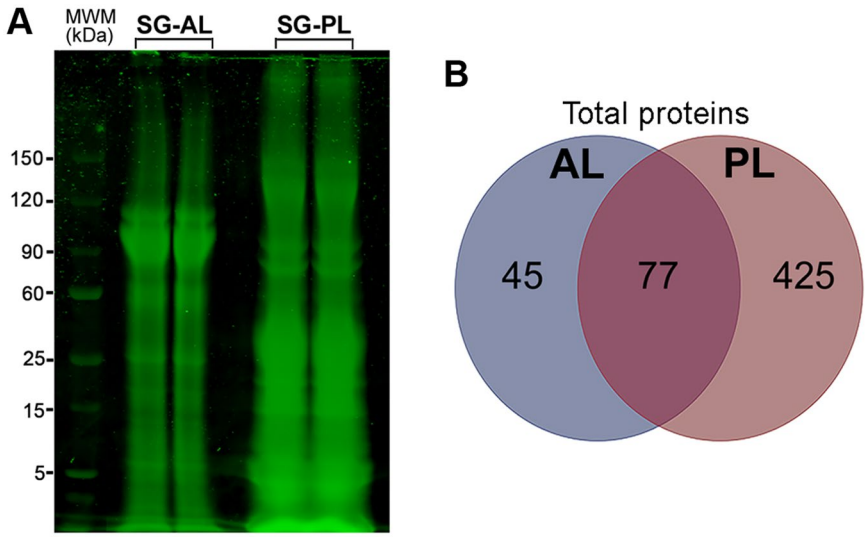

Figure 3. Proteomics analysis of *Charonia tritonis* anterior lobe (AL) and posterior lobe (PL) of the salivary gland (SG). (**A**) SDS-PAGE and Coomassie stain of extracts derived from the SG-AL and SG-PL. (**B**) Comparison of total proteins identified in extracts of SG-AL and SG-PL, based on Pfam analysis.

family database): 122 and 502 Pfam families were identified from SG-AL and SG-PL, respectively, with 77 families common to both (Fig. 3B).

Supplementary Data S7 provides a summary of the MS analysis of the SG-AL and SG-PL extracts. Proteins that were highly represented in MS analysis for either or both the SG-AL and SG-PL, are shown in Table 1. In the *C. tritonis* SG-PL, the most highly represented protein was the lectin L6-like protein. Glycan-binding proteins, commonly known as lectins, play a crucial role in innate (and adaptive) immunity. Binding of potential pathogens by lectins leads to phagocytosis, complement activation, and antigen processing but also to regulation of adaptive immune functions[59,60]. In addition to their role in pathogen recognition, some lectins act as direct defense effectors by intoxicating the antagonist upon binding[61]. In the SG-AL, the most highly represented protein was aminopeptidase N, suggesting high abundance in this lobe. Aminopeptidase N is widely distributed in both plant and animal species where it is known to selectively break down amino acids from the amino-terminus of proteins or oligopeptides[62]. In animals, this enzyme is most abundant along the brush border membrane of the intestines, facilitating the digestion of ingested protein[63]. However, in the midgut of insects, the enzyme can act as a receptor binding to toxin proteins produced by viruses and bacteria[64–66].

The hemorrhagic metalloprotease disintegrin-like proteins and cysteine-rich secretory Mr30 were also highly represented in our MS analysis (Table 1). Hemorrhagic metalloprotease disintegrin-like proteins have been isolated from snake venom where have been shown to inhibit the process of collagen- and ADP-induced platelet aggregation[67], break-down of coagulation factors and the initiation of apoptosis[68]. The cysteine-rich secretory Mr30 has been identified from *Conus* snails and reported to have similar properties to Tex31, a protease responsible for processing of pro-conotoxins[69,70]. The *C. tritonis* SG does not contain conotoxins, yet the cysteine-rich secretory Mr30 may help to pre-process other types of pro-toxin proteins, including the venom serine carboxypeptidase, a member of the peptidase S10 family. This enzyme is known to have various physiological functions, including enhancing massive release of histamine, degradation of neurotransmitters, mediation of immunity-related processes, phosphorylation of venom proteins, and influencing the nervous system as a neurotoxic polypeptide[71]. The biological role of this peptidase in *C. tritonis* venom is unclear, but given that members of the peptidase S10 family are active at acidic pH[72], they may perform their function in the venom before it is injected into the prey.

Arylsulfatase hydrolyses the sulfate group of ingested biomolecules, such as glycosaminoglycans (GAGs), which are large sugar molecules[73,74]. In molluscs, arylsulfatase activity has been reported in various tissues of ivory barnacles (*Balanus eburneus*), including the mantle, suggesting a probable relationship between arylsulfatase activity and the cyclic formation and hardening of the exoskeleton[75]. In snails of the family Muricidae, arylsulfatase is found in the hypobranchial gland where it plays a role in Tyrian purple biosynthesis[76]; it helps in the conversion of tyrindoxyl sulphate into the biologically active precursors of Tyrian purple[77,78].

A single arylsulfatase was identified in the *C. tritonis* SG-AL through proteomic analysis, although another 29 transcripts were present in the transcriptomes that encode for arylsulfatases. No arylsulfatase proteins were identified in the SG-PL; however, 36 transcripts were identified that encode for arylsulfatases. This finding provides further evidence that arylsulfatase genes are encoded within the animal's genome, rather than being obtained from dietary sources or through symbiotic microorganisms, as has been suggested from other molluscan studies[79,80]. It is speculated that SG arylsulfatase is involved in the breakdown of prey biomolecules during feeding. Echinoderms are well known to contain a diverse array of saponin molecules (to deter predators, parasites and microbes) including sulfated saponins; this subclass may be neutralized or broken down by arylsulfatase-mediated hydrolysis depending on the position of sulfation on either the aglycone or sugar moiety[81]. *C. tritonis* arylsulfatases contain all conserved arylsulfatase domains, and besides a variable signal sequence, the mature enzyme is highly conserved with arylsulfatases from five other species (*Aplysia californica*, *Octopus bimaculosides*, *Helix pomatia*, *Biomphalaria glabrata* and *Strongylocentrotus purpuratus* (Fig. 4).

We report the identification of putative toxin-related proteins from the transcriptome, with some being supported by the proteome MS identification, as shown in Table 2; their gene expression level (RPKM) is provided in Supplementary Data S8.

The cysteine-rich venom proteins (CRVPs) belong to the larger family of proteins known as the cysteine-rich secretory proteins (CRISPs), and are found in the venoms of diverse species, including snakes, cone snails, coleoids, stinging insects, scorpions and spiders[82–88]. Proteins from this family are also commonly found in the mammalian male reproductive tract[89] and are associated with a broad range of functions, such as fertilization and sperm-egg interaction[86,88]. In the current study, 8 transcripts that encode venom-like CRISPs were identified within the SG-AL, and 2 were confirmed through proteomic analysis (Table 2). In addition, 3 transcripts that encode venom-like CRISPs were identified from the SG-PL, and an additional 2 confirmed through proteomics analysis (Table 2). Domain analysis predicts regions characteristic of CRISPs, including the first class of pathogenesis-related proteins (Pr-1) and a cysteine-rich domain (CRD) (Fig. 4)[90]. Multiple sequence alignment with CRISPs from 2 other species, *Conus textile* and *Conus marmoreus*, showed that there is a high level of diversity in *C. tritonis* venom-like CRISPs, besides spatial arrangement of cysteine (C) residues (Fig. 4). CRVPs are well known to exert multiple activities through the blocking of L-type Ca^{2+} channels and K^{+} channel inhibitors[87], which can reduce smooth muscle contraction and cause myonecrosis. Recent studies have revealed that CRISPs in snake venoms inhibit smooth muscle contraction and cyclic nucleotide-gated ion channels[83]. Considering that the CRISPs found in the venom of snakes could function as ion channel blockers[91,92], the triton CRISPs might have a similar function by targeting the ion channels of prey.

Metalloproteinases are a family of proteolytic enzymes that are involved in a large number of biological processes. A variety of metalloproteinases are found in the venoms of spiders, scorpions, centipedes, cone snails and the platypus[93–98]. In snakes, these enzymes cause hemorrhaging upon envenomation[99]. The biochemical basis for metalloproteinase activity is through proteolytic destruction of tissue basement membranes and of the extracellular matrix surrounding capillaries and small vessels. They may also interfere with coagulation, thus

AL	PL	AL	PL		AL	PL	AL	PL	
Transcriptome		Proteome		Best BLAST match	Transcriptome		Proteome		Best BLAST match
✓	✓	×	21	4-hydroxyphenylpyruvate dioxygenase	✓	✓	×	28	Filamin-A-like isoform X1
✓	✓	×	20	4-hydroxyphenylpyruvate dioxygenase	✓	✓	×	25	Filamin-C-like isoform X1
✓	✓	14	✓	78 kDa glucose-regulated	×	✓	×	51	Fish-egg lectin-like
✓	×	13	✓	A disintegrin and metalloase with thrombospondin motifs 18	✓	✓	×	19	Fructose-bisphosphate aldolase 1
✓	✓	29	✓	A disintegrin and metalloase with thrombospondin motifs 20-like	✓	✓	×	18	Fructose-bisphosphate aldolase 1
✓	✓	×	42	Actin	✓	✓	×	17	Fructose-bisphosphate aldolase 1
✓	✓	×	38	Actin	✓	✓	58		Galactose-1-phosphate uridylyltransferase
✓	✓	×	36	Actin	✓	✓	21	17	GLIPR1 1
✓	✓	14		ADAM family mig-17-like	✓	✓	20	17	GLIPR1 1
✓	✓	×	19	Advillin	✓	✓	×	19	Glyceraldehyde-3-phosphate dehydrogenase
✓	✓	×	19	Advillin	✓	✓	×	19	Heat shock 70
✓	✓	×	17	Alpha-enolase isoform X1	✓	✓	×	18	Heat shock 70
✓	✓	×	16	Alpha-enolase isoform X1	✓	✓	×	57	Hemocyanin isoform 1
✓	✓	54	×	Aminopeptidase N	✓	✓	×	38	Hemocyanin isoform 1
✓	✓	51	×	Aminopeptidase N	✓	✓	×	33	Hemocyanin isoform 1
✓	✓	28	×	Aminopeptidase N	✓	✓	×	38	Hemocyanin isoform 2
✓	✓	26	×	Aminopeptidase N	✓	×	33	×	Hemorrhagic metallo ase-disintegrin-like kaouthiagin isoform X1
✓	✓	20	×	Aminopeptidase N	✓	✓	25	×	Hepatic lectin-like
✓	✓	18	×	Aminopeptidase N	✓	×	15	×	Hypothetical protein LOTGIDRAFT_174864
✓	✓	17	×	Aminopeptidase N	✓	✓	×	59	Lectin L6-like
✓	✓	16	×	Aminopeptidase N	✓	✓	×	18	Lectin L6-like
✓	✓	13	×	Aminopeptidase N	✓	✓	×	18	Lectin L6-like
✓	✓	13	×	Aminopeptidase N	✓	✓	21	×	Mast cell carboxypeptidase A
✓	✓	100	×	Aminopeptidase N isoform X2	✓	×	13	×	MAX gene-associated
✓	✓	24	×	Aminopeptidase N-like	✓	✓	×	20	MAX gene-associated
✓	✓	23	×	Aminopeptidase N-like	✓	✓	75	×	Mucin-19-like isoform X3
✓	✓	17	×	Aminopeptidase N-like	✓	✓	×	25	Myosin heavy chain
✓	✓	17	×	Arylsulfatase B	✓	✓	×	22	Myosin heavy chain
✓	✓	20	44	Arylsulfatase B-like	✓	✓	×	34	Myosin heavy chain isoform A
✓	✓	15	58	Arylsulfatase B-like	✓	✓	×	25	Neuroendocrine convertase 1
✓	✓	14	×	Arylsulfatase B-like	✓	✓	×	19	Neuroendocrine convertase 1
✓	✓	×	24	Cartilage matrix -like	✓	✓	×	22	Paramyosin
✓	✓	×	21	Cartilage matrix -like	✓	✓	×	21	Paramyosin
✓	✓	×	20	Cartilage matrix -like	✓	✓	×	26	Paramyosin-like isoform X2
✓	✓	×	15	Cartilage matrix -like	✓	✓	20	×	Probable palmitoyltransferase ZDHHC4
✓	✓	×	15	Cartilage matrix -like	✓	✓	26	×	Probable serine carboxypeptidase CPVL
✓	×	20	×	Cholinesterase	✓	✓	19	×	Probable serine carboxypeptidase CPVL
✓	×	13	×	C-type lectin domain family member A isoform X1	✓	✓	40	×	Retinal degeneration B-like isoform X1
✓	✓	29	×	Cysteine-rich secretory Mr30	✓	✓	30	×	Ribonuclease Z
✓	✓	23	×	Cysteine-rich secretory Mr30	✓	✓	30	×	Ribosomal S6 kinase 2 alpha
✓	✓	×	18	Disulfide isomerase	✓	×	18	×	Serine protease 33-like isoform X2
✓	✓	18	61	Endoglucanase 4-like	✓	✓	×	26	Tropomyosin
✓	✓	17	71	Endoglucanase A-like	✓	✓	×	17	Tubulin beta-4B chain
✓	✓	28	×	Endoplasmic reticulum aminopeptidase 1	✓	✓	×	17	Twitchin isoform X18
✓	✓	63	×	Endoplasmic reticulum aminopeptidase 2	✓	✓	15	×	Venom serine carboxypeptidase
✓	✓	×	51	Filamin-A-like isoform X1	✓	×	24	×	Venom serine carboxypeptidase CPVL
✓	✓	×	30	Filamin-A-like isoform X1	✓	×	23	×	Venom serine carboxypeptidase CPVL
					✓	×	26	×	Zinc metallo ase-disintegrin-like VLAIP-A

Table 1. Proteins identified in the anterior lobe (AL) and posterior lobe (PL) of the *Charonia tritonis* salivary gland (SG). (✓) Represents identified, and (×) represents not identified. Numbers represent number of peptide sequences from the proteomic analyses that match to the transcriptome.

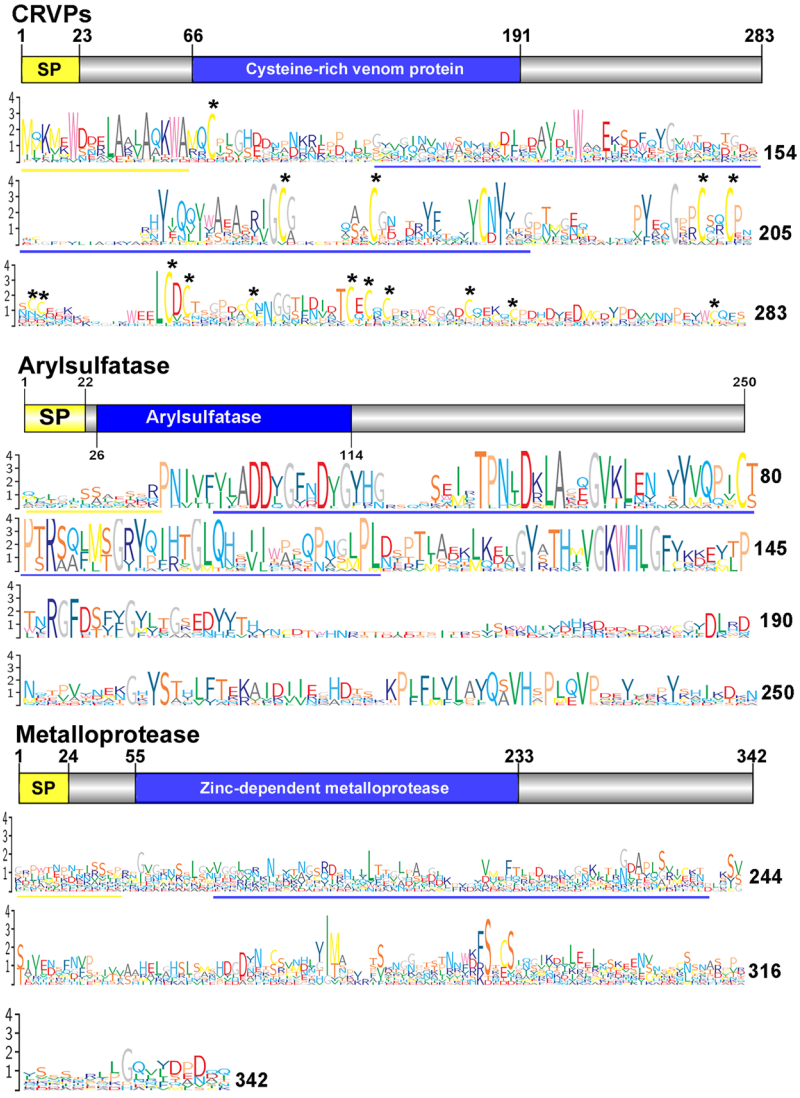

Figure 4. Molecular characterisation of *Charonia tritonis* cysteine-rich venom proteins (CRVPs), arylsulfatase and metalloprotease. Schematic diagram (top) showing the general organization with signal peptide (SP) and conserved domains (blue). Sequence logo representation (below) of multiple sequence alignments for *C. tritonis* with other species (Supplementary Data S8). Asterisks represent site of conserved cysteine (C) residues. Region of signal peptide (yellow) and conserved domain (blue) are shown.

Annotation	SG Transcriptome	SG-AL Transcriptome/ Proteome	SG-PL Transcriptome/ Proteome
Cysteine-rich venom protein	11	8/2	3/2
Snake venom metalloproteinase-like	9	3/1	6/2
Echotoxin	2	2/0	2/0
Venom Carboxylesterase-6	2	2/0	0/0
Venom serine carboxypeptidase	9	4/0	5/2

Table 2. Identification of putative toxin-related proteins from the *Charonia tritonis* salivary gland (SG) anterior lobe (AL) and posterior lobe (PL).

complementing loss of blood from the vasculature. The variety of hemorrhagic toxins found in snake venoms is due to the presence of structurally related proteins composed of various domains[99]. The type of domains found in each toxin plays a major role in the hemorrhagic potency of the protein.

Three transcripts were identified that encode venom-related metalloproteinases in the *C. tritonis* SG-AL with a single zinc metalloproteinase confirmed by proteome analysis. In the SG-PL, seven transcripts were found which

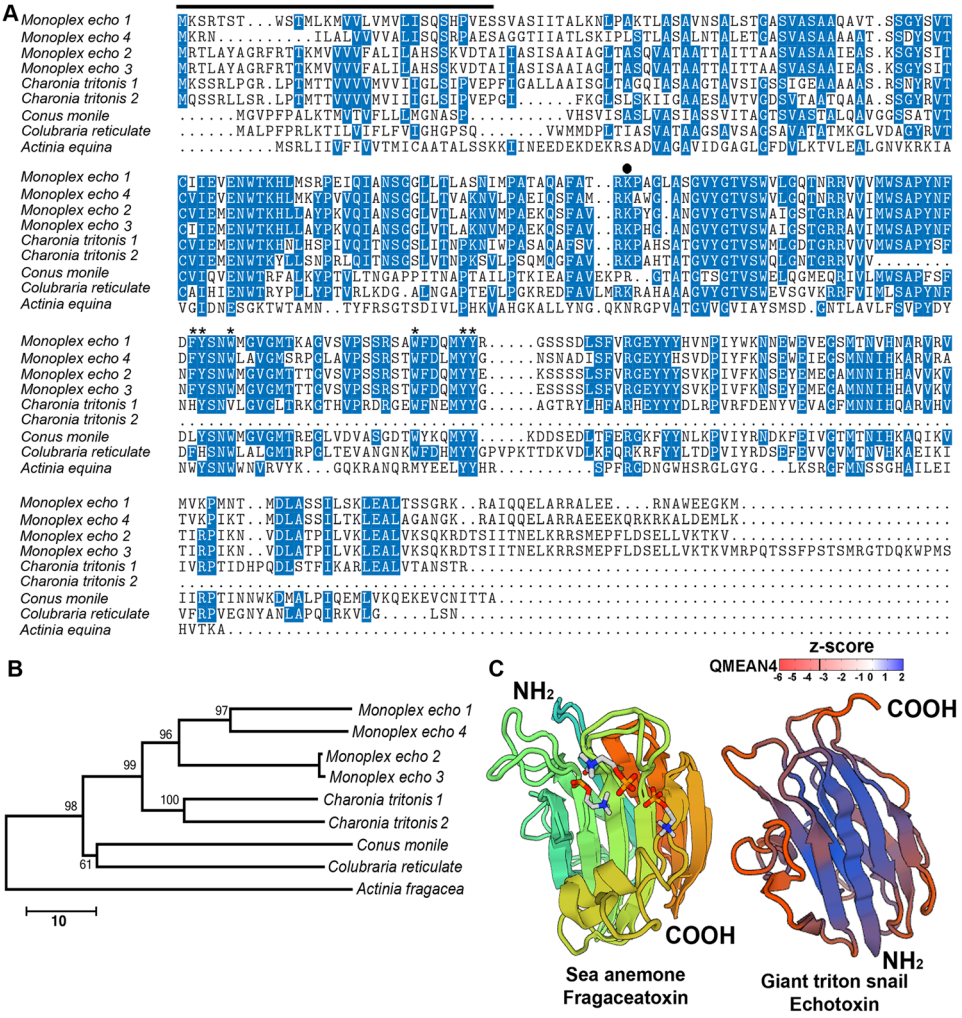

Figure 5. Molecular characterization of *Charonia tritonis* echotoxin proteins. (**A**) Multiple sequence alignment of *C. tritonis* echotoxin and with echotoxins from other species. Genbank accession numbers for all proteins are provided in Supplementary Data S8. Shading represents high amino acid conservation and the line shows region of signal peptide based on *M. echo*. The Lys (K) residue and residues involved in the aromatic patch are indicated by a closed circle and asterisks, respectively. (**B**) Phylogenetic tree of echotoxin proteins using neighbor-joining estimation. Scale bar represents amino acid substitutions. (**C**) 3D structure of fragaceatoxin from sea anemone (SWISS-MODEL id: 4tsn.3.A; identity 22.68% and sequence similarity 0.32) and the predicted *C. tritonis* echotoxin model, shown using ribbon representation in DeepView. Analysis of Z-scores of the template protein (fragaceatoxin) and echotoxin from *C. tritonis* shows the geometrical features responsible for an observed negative value. Large negative values correspond to red regions in the color gradient, and light red and deep blue region represents maximum match with protein used for modelling and the experimental protein. The structure reveals up to one ligand (phosphocholine) bound to a single chain of fragaceatoxin, a single binding site is also present in the echotoxin of *C. tritonis*.

encode for metalloproteinase proteins and two proteins in the *in silico* exoproteome analysis. The zinc-dependent metalloproteinase contains a conserved metalloproteinase domain (Fig. 4). Multiple sequence alignment shows the conservation of cysteines and glycosaminoglycan attachment sites (serine motifs) in *C. tritonis*-derived metalloproteineases with four other species i.e. *Lottia gigantea*, *Crassostrea gigas*, *Biomphalaria glabrata* and *Octopus bimaculoides*. In the parasitic wasp *Chelonus inanitus*, conservation of high number of serine motifs is thought to be involved in substrate or site specific binding of venom protein[100]. This group of metalloproteineases belong to the MEROPS peptidase family M12, subfamily M12B [adamalysin family, clan (MA(M))]. The adamalysins are zinc-dependent endopeptidases also found in snake venom. The 'A disintegrin and metalloprotease' (ADAM) family of metalloproteases (also referred to as adamalysin-like metalloproteases) contains proteolytic domains from snake venoms, proteases from the mammalian reproductive tract, and the tumor necrosis factor alpha convertase, TACE. ADAMs are glycoproteins, which are involved in cell signaling, cell fusion, and cell-cell interactions. This supports a role for *C. tritonis* salivary gland metalloproteinase in defense, although further study is required to define its function.

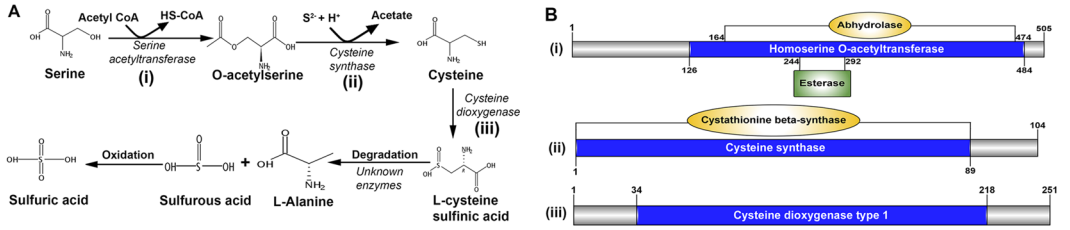

Figure 6. Identification of enzymes associated with the sulfuric acid biosynthesis pathway. (**A**) Pathway for biosynthesis of sulfuric acid. Those enzymes identified within the anterior lobe of the *Charonia tritonis* salivary gland are shown as (i), (ii) and (iii). (**B**) Schematics showing enzymes (i), (ii) and (iii) including characteristic domains. Biosynthetic enzymes derived from *C. tritonis* are listed in Supplementary Data S8.

Echotoxins (1, 2 and 3) are lethal and hemolytic proteinaceous toxins of approximately 25 kDa, which were identified from the SG of the Tonnoidea, *Monoplex echo*[44, 101, 102]. Other echotoxins were subsequently identified in non-Tonnoidea snails through transcriptomics analysis of *Conus consors* and *Conus geographus* (superfamily Conoidea)[103, 104], as well as the *C. reticulate* (superfamily Buccinoidea)[6]. In this study, two deduced echotoxin-like proteins were identified from *C. tritonis*, present in both the SG-AL and SG-PL, at 275 residues (full-length) and 142 residues (partial-length). Multiple sequence alignment of known species echotoxins shows high conservation throughout the entire precursor besides the N- and C-terminal regions (Fig. 5A). No N-terminal signal peptide was predicted for either *C. tritonis* echotoxin-like proteins (based on SignalP analysis), yet alignment with *M. echo* echotoxins suggests that a signal peptide would be cleaved following V_{30}EP. Of the 6 aromatic residues that are thought to form an aromatic patch on the surface of these types of protein[105], 4 are conserved in the *C. tritonis* echotoxin-like protein. Also, a lysine residue, which is predicted to be involved in the assembly of actinoporin molecules for pore-formation to lipid membranes[105], is present. A phylogenetic analysis supports, with high confidence, the evolutionary origin of *M. echo* echotoxins being most closely related to *C. tritonis* (Fig. 5B).

Echotoxins lyse erythrocytes following binding to gangliosides, which is a similar mechanism to that of some bacterial hemolysins[106], yet dissimilar to the marine hemolysins, for example, sea anemone hemolysins bind to sphingomonnyelin[107]. Sea anemones are a rich source of lethal pore-forming toxins (PFTs) that may include a combination of peptides and proteins, known as cytolysins or actinoporins[108]. PFTs target cell membranes forming water-filled pores across the lipid bilayer, followed by oligomerization and penetration of the protein subunits through the lipid bilayer. The discovery of actinoporin-like hemolysins (echotoxins) within higher eumetazoans is of particular interest in comparative biochemistry. However, it should be noted that echotoxins and actinoporins have distinct modes of action[101, 107]. Interestingly, a sequence homology search using *C. tritonis* echotoxins revealed some similarity (a three-turn alpha helix and beta sheet) with fragaceatoxin, an actinoporin-type of pore forming hemolytic protein from sea anemone (SWISS-MODEL ID: 4tsn.3.A) (Fig. 5C). The crystal structures of two other actinoporin proteins from sea anemone, equinotoxin II and sticholysin II, both revealed a compact beta-sandwich consisting of ten strands in two sheets flanked on each side by two short alpha-helices, which is a similar topology to osmotin, a plant defense protein belonging to the fifth class of the pathogenesis-related proteins (Pr-5)[109, 110]. Studies have reported that the beta sandwich structure attaches to the membrane, while a three-turn alpha helix lying on the surface of the beta sheet may be involved in membrane pore formation, possibly via the penetration of the membrane by the helix[109–112]. Additionally, computer-aided protein structure prediction identified a ligand-binding site for phospohocholine on *C. tritonis* echotoxin (Fig. 5C). In sea anemone, small and basic α-pore forming actionporin proteins have a phosphocholine binding site which facilitates binding to the cell membrane and formation of pores, a feature that they share with toxins such as diphtheria and anthrax[111]. The identification of echotoxins from *C. tritonis* suggests a broad role for these in marine gastropod snails, and are most likely important for prey interaction.

Analysis of sulfuric acid biosynthesis enzyme genes. Many marine gastropod snails, for the purpose of feeding and defense, release strong acids[20, 21, 113–116]. Although acids can facilitate penetration through the prey calcareous body wall, the acids can also serve as an allomone through their action to deter epibiont fouling, kill/traumatize their prey or avoid predation[112]. Several research studies within the molluscan Pleurobranchoidea family (commonly known as sea slugs) have focused on sulfuric acid production through histochemistry, showing large acid vacuoles in the median buccal gland and the subepithelial glands[113, 116, 117].

In the Tonnoidea superfamily, acid production in several families, including the Ranellidae and Cassidae, has been investigated[32]. For example, in the family Ranellidae, extracts of the SG-PL of *Cymatium lampas* induced immediate paralysis in the sea star *Patriella brevispina*[35]. The PL-SGs of *Cymatuim intermedius* and *Gyrineum natator* both contain specialized acid-producing and protein-secreting epithelial cells and secrete strong acids[20, 21, 114]. *G. natator* uses sulfuric acid produced in the salivary glands to make holes in the oyster shells and also uses these secretions to attack prey only when more easily obtained food is not available[32]. These marine gastropods can also use these acid secretions for their defense[30, 32, 33]. In *Charonia* species, saliva secreted from *C. tritonis* putatively immobilizes COTS[35]. However, previous studies were unable to identify the chemical components of secreted saliva from *Charonia* sp. salivary gland; *C. lampas* did not inject venom or acid into its prey but rather used its foot to capture and manipulate the prey and its radula to consume the flesh[30].

Cysteine biosynthesis genes were found in the *C. tritonis* SG-AL and the *in silico* exoproteome analysis (Supplementary Data S2a). Proteomics analysis revealed one arylsulfatase B-like protein Arylsulfatase, a sulfur

scavenging enzyme, which may play a role in the breakdown of sulphated saponins[81]. Presence of a higher level of arylsulfatase in the digestive organs of the predatory mollusks has been reported[118]. It has also been confirmed that this enzyme catalyzed cleavage of sulfate in the C-4 position of xylose incorporated into carbohydrate chains of saponins from sea cucumbers[81]. In triton snail, after breakdown of saponin by arylsulfatase, released sulfates may be processed in the SG-AL to synthesize sulphuric acid. Three major enzymes required for the biosynthesis of sulfuric acids, serine acetyltransferase, cysteine synthase and cysteine dioxygenase, have been found in *C. tritonis* (Fig. 6A) and domain conservation for those enzymes in SG-AL tissue subsequently identified (Fig. 6B). Although the present study reveals the genetic metabolic tools required for biosynthesis of sulfuric acids in the SG-AL, further studies are necessary to confirm its production.

Conclusions

We have described through analysis of tank assays the process involved in *C. tritonis* attack on COTS, including proboscis extension, penetration, and the likely secretion of SG-derived feeding and putative toxin-related proteins. Transcriptome and proteome analysis of the SG-AL and SG-PL have identified putative venom- and feeding-related proteins. This work provides insight into the source of bioactive components used by *C. tritonis* to predate on COTS.

Data Accessibility. Raw sequence data for transcriptome assemblies can be found at NCBI PRJNA383875. Protein sequences for all species proteins used in this investigation are provided in File S8.

References

1. Remigio, E. & Duda, T. F. Evolution of ecological specialization and venom of a predatory marine gastropod. *Mol Ecol.* **17**, 1156–1162 (2008).
2. Russell, F. E. Marine toxins and venomous and poisonous marine plants and animals (invertebrates). *Adv Mar Biol.* **21**, 59–217 (1984).
3. Margres, M. J., Aronow, K., Loyacano, J. & Rokyta, D. R. The venom-gland transcriptome of the eastern coral snake (*Micrurus fulvius*) reveals high venom complexity in the intragenomic evolution of venoms. *BMC Genomics* **14**, 1 (2013).
4. Olivera, B. M., Rivier, J., Scott, J., Hillyard, D. & Cruz, L. Conotoxins. *J Biol Chem.* **266**, 22067–22070 (1991).
5. Halai, R. & Craik, D. J. Conotoxins: natural product drug leads. *Nat Prod Rep.* **26**, 526–536 (2009).
6. Modica, M. V., Lombardo, F., Franchini, P. & Oliverio, M. The venomous cocktail of the vampire snail *Colubraria reticulata* (Mollusca, Gastropoda). *BMC genomics* **16**, 441 (2015).
7. Kodama, M. *et al*. Tetrodotoxin secreting glands in the skin of puffer fishes. *Toxicon* **24**, 819–829 (1986).
8. Freeman, S. E. & Turner, R. Maculotoxin, a potent toxin secreted by *Octopus maculosus* Hoyle. *Toxicol Appl Pharmacol.* **16**, 681–690 (1970).
9. Brinkman, D. L. *et al*. Transcriptome and venom proteome of the box jellyfish *Chironex fleckeri*. *BMC Genomics.* **16**, 1 (2015).
10. Tachibana, K. *et al*. Okadaic acid, a cytotoxic polyether from two marine sponges of the genus Halichondria. *J Am Chem Soc.* **103**, 2469–2471 (1981).
11. Lucas, J., Hart, R., Howden, M. & Salathe, R. Saponins in eggs and larvae of *Acanthaster planci* (L.)(Asteroidea) as chemical defences against planktivorous fish. *J Exp Mar Bio Ecol.* **40**, 155–165 (1979).
12. Casewell, N. R., Wüster, W., Vonk, F. J., Harrison, R. A. & Fry, B. G. Complex cocktails: the evolutionary novelty of venoms. *Trends Ecol Evol.* **28**, 219–229 (2013).
13. Olivera, B. M., Showers Corneli, P., Watkins, M. & Fedosov, A. Biodiversity of cone snails and other venomous marine gastropods: evolutionary success through neuropharmacology. *Annu Rev Anim Biosci.* **2**, 487–513 (2014).
14. Kaas, Q., Yu, R., Jin, A.-H., Dutertre, S. & Craik, D. J. ConoServer: updated content, knowledge, and discovery tools in the conopeptide database. *Nucleic Acids Res.* **40**, 325–330 (2011).
15. Prashanth, J. R., Lewis, R. J. & Dutertre, S. Towards an integrated venomics approach for accelerated conopeptide discovery. *Toxicon* **60**, 470–477 (2012).
16. Dutertre, S. *et al*. Evolution of separate predation-and defence-evoked venoms in carnivorous cone snails. *Nat Comm*. **5** (2014).
17. Robinson, S. D. *et al*. Hormone-like peptides in the venoms of marine cone snails. *Gen Comp Endocrinol.* **244**, 11–18 (2017).
18. Fänge, R. in *Toxins, Drugs, and Pollutants in Marine Animals* (eds Bolis, L., Zadunaisky, J. & Gilles, R.) 47–62 (Springer, 1984).
19. Hughes, R. & Hughes, H. Morphological and ehavioural aspects of feeding in the *Cassidae*(Tonnacea, Mesogastropoda). *Malacologia* **20**, 385–402 (1981).
20. West, D. J., Andrews, E. B., McVean, A. R., Thorndyke, M. C. & Taylor, J. D. Presence of a toxin in the salivary glands of the marine snail *Cymatium intermedius* that targets nicotinic acetylcholine receptors. *Toxicon.* **36**, 25–29 (1998).
21. Andrews, E. B., Page, A. & Taylor, J. The fine structure and function of the anterior foregut glands of *Cymatium intermedius* (Cassoidea: Ranellidae). *J Molluscan Stud.* **65**, 1–19 (1999).
22. Schroeder, R. Urchin killer. *Sea Front* **8**, 156–160 (1962).
23. Snyder, N. & Snyder, H. Alarm response of *Diadema antillarum*. *Science.* **168**, 276–278 (1970).
24. Houbrick, J. R. & Fretter, V. Some aspects of the functional anatomy and biology of Cymatium and Bursa. *J Molluscan Stud* **38**, 415–429 (1969).
25. Fänge, R. & Lidman, U. Secretion of sulfuric acid in *Cassidaria echinophora* Lamarck (Mollusca: Mesogastropoda, marine carnivorous snail). *Comp Biochem Physiol A Comp Physiol* **53**, 101–103 (1976).
26. Wilson, B. & Gillett, K. *Australian shells, (revised edn)*. (1974).
27. Chesher, R. H. Destruction of Pacific corals by the sea star *Acanthaster planci*. *Science.* **165**, 280–283 (1969).
28. Poulsen, A. L. Coral reef gastropods-a sustainable resource? *Pacific Conserv Biol* **2**, 142–145 (1995).
29. Kang, K. H. & Kim, J. M. The predation of trumpet shell, *Charonia* sp., on eight different marine invertebrate species. *Aquaculture Res* **35**, 1202–1206 (2004).
30. Morton, B. Foregut anatomy and predation by *Charonia lampas* (Gastropoda: Prosobranchia: Neotaenioglossa) attacking *Ophidiaster ophidianus* (Asteroidea: Ophidiasteridae) in the Açores, with a review of triton feeding behaviour. *J Nat History* **46**, 2621–2637 (2012).
31. Hall, M. R. *et al*. The Crown-of-Thorns starfish genome as a tool for biocontrol of a coral reef pest. *Nature* **544**, 231–234 (2017).
32. Morton, B. The feeding strategy of the predatory Gyrineum natator (Gastropoda: Neotaenioglossa: Ranellidae) in the Cape d'Aguilar Marine Reserve, Hong Kong, with a review of sulphuric acid use in prey access by the Tonnoidea and experimentally derived estimates of consumption. *J Nat History* **49**, 483–507 (2015).
33. Morton, B. Prey capture, preference and consumption *Bylinatella caudata* (Gastropoda: Tonnoidea: Ranellidae) in Hong Kong. *J Molluscan Stud* **56**, 477–486 (1990).

34. Bandel, K. The radulae of Caribbean and other Mesogastropoda and Neogastropoda. 1–199 (EJ Brill, 1984).
35. Endean, R. Aspects of molluscan pharmacology. *Chem Zool* **7**, 421–466 (1972).
36. Barkalova, V. O., Fedosov, A. E. & Kantor, Y. I. Morphology of the anterior digestive system of tonnoideans (Gastropoda: Caenogastropoda) with an emphasis on the foregut glands. *Molluscan Res.* **36**, 54–73 (2016).
37. Shiomi, K., Mizukami, M., Shimakura, K. & Nagashima, Y. Toxins in the salivary gland of some marine carnivorous gastropods. *Comp Biochem Physiol B Biochem Mol Biol* **107**, 427–432 (1994).
38. Shiomi, K., Midorikawa, S., Ishida, M., Nagashima, Y. & Nagai, H. Plancitoxins, lethal factors from the crown-of-thorns starfish *Acanthaster planci*, are deoxyribonucleases II. *Toxicon.* **44**, 499–506 (2004).
39. Min, X. J., Butler, G., Storms, R. & Tsang, A. OrfPredictor: predicting protein-coding regions in EST-derived sequences. *Nucleic Acids Res* **33**, W677–W680 (2005).
40. Schwanhäusser, B. *et al*. Global quantification of mammalian gene expression control. *Nature.* **473**, 337–342 (2011).
41. Liu, W. *et al*. IBS: an illustrator for the presentation and visualization of biological sequences. *Bioinformatics* **31**, 3359–3361 (2015).
42. Tamura, K., Stecher, G., Peterson, D., Filipski, A. & Kumar, S. MEGA6: molecular evolutionary genetics analysis version 6.0. *Mol Biol Evol* **30**, 2725–2729 (2013).
43. Biasini, M. *et al*. SWISS-MODEL: modelling protein tertiary and quaternary structure using evolutionary information. *Nucleic Acids Res* **42**, W252–W258 (2014).
44. Kawashima, Y., Nagai, H., Ishida, M., Nagashima, Y. & Shiomi, K. Primary structure of echotoxin 2, an actinoporin-like hemolytic toxin from the salivary gland of the marine gastropod *Monoplex echo*. *Toxicon* **42**, 491–497 (2003).
45. Petersen, T. N., Brunak, S., von Heijne, G. & Nielsen, H. SignalP 4.0: discriminating signal peptides from transmembrane regions. *Nature methods* **8**, 785–786 (2011).
46. Hiller, K., Grote, A., Scheer, M., Munch, R. & Jahn, D. PrediSi: prediction of signal peptides and their cleavage positions. *Nucleic acids research* **32**, W375–379, doi:10.1093/nar/gkh378 (2004).
47. Krogh, A., Larsson, B., von Heijne, G. & Sonnhammer, E. L. Predicting transmembrane protein topology with a hidden Markov model: application to complete genomes. *Journal of molecular biology* **305**, 567–580, doi:10.1006/jmbi.2000.4315 (2001).
48. Schultz, J., Milpetz, F., Bork, P. & Ponting, C. P. SMART, a simple modular architecture research tool: identification of signaling domains. *Proc Natl Acad Sci USA* **95**, 5857–5864 (1998).
49. Gupta, R., Jung, E. & Brunak, S. *Prediction of N-glycosylation sites in human proteins*, http://www.cbs.dtu.dk/services/NetNGlyc/ (2004).
50. Wang, T. *et al*. Proteomic Analysis of the *Schistosoma mansoni* Miracidium. *PloS one.* **11**, e0147247 (2016).
51. Cummins, S. F. & Bowie, J. H. Pheromones, attractants and other chemical cues of aquatic organisms and amphibians. *Nat Prod Rep* **29**, 642–658 (2012).
52. Nugranad, J., Chantrapornsilp, S. & Varapibal, T. Feeding and spawning behaviour of the trumpet triton, *Charonia tritonis* (L., 1758) in captivity. *Phuket Mar Biol Center Special Publ* **21**, 51–56 (2000).
53. Mackie, A., Singh, H. & Fletcher, T. Studies on the cytolytic effects of seastar (*Marthasterias glacialis*) saponins and synthetic surfactants in the plaice *Pleuronectes platessa*. *Mar Biol.* **29**, 307–314 (1975).
54. Aguiar, R. & Wink, M. How do slugs cope with toxic alkaloids? *Chemoecology.* **15**, 167–177 (2005).
55. Bowyer, P., Clarke, B., Lunness, P., Daniels, M. & Osbourn, A. Host range of a plant pathogenic fungus determined by a saponin detoxifying enzyme. *Science.* **267**, 371 (1995).
56. Bouarab, K., Melton, R., Peart, J., Baulcombe, D. & Osbourn, A. A saponin-detoxifying enzyme mediates suppression of plant defences. *Nature.* **418**, 889–892 (2002).
57. Day, J. A. Feeding of the cymatiid gastropod, *Argobuccinum argus*, in relation to the structure of the proboscis and secretions of the proboscis gland. *Am Zool* **9**, 909–916 (1969).
58. Chun, J. B. *et al*. Cone snail milked venom dynamics–a quantitative study of Conus purpurascens. *Toxicon* **60**, 83–94 (2012).
59. Vasta, G. R., Ahmed, H., Tasumi, S., Odom, E. W. & Saito, K. Biological roles of lectins in innate immunity: molecular and structural basis for diversity in self/non-self recognition. *Adv Exp Med Biol* **598**, 389–406 (2007).
60. Saito, T., Kawabata, S.-i, Hirata, M. & Iwanaga, S. A novel type of limulus lectin-L6. *Purification, primary structure, and antibacterial activity. J Biol Chem* **270**, 14493–14499 (1995).
61. Wohlschlager, T. *et al*. Methylated glycans as conserved targets of animal and fungal innate defense. *Proc Natl Acad Sci USA* **111**, E2787–E2796 (2014).
62. Nakanishi, K. *et al*. Aminopeptidase N isoforms from the midgut of *Bombyx mori* and *Plutella xylostella*–their classification and the factors that determine their binding specificity to *Bacillus thuringiensis* Cry1A toxin. *FEBS Lett* **519**, 215–220 (2002).
63. Knight, P. J., Crickmore, N. & Ellar, D. J. The receptor for *Bacillus thuringiensis* CrylA (c) delta-endotoxin in the brush border membrane of the lepidopteran *Manduca sexta* is aminopeptidase N. *Mol Microbiol.* **11**, 429–436 (1994).
64. Rajagopal, R., Sivakumar, S., Agrawal, N., Malhotra, P. & Bhatnagar, R. K. Silencing of midgut aminopeptidase N of *Spodoptera litura* by double-stranded RNA establishes its role as *Bacillus thuringiensis* toxin receptor. *J Biol Chem* **277**, 46849–46851 (2002).
65. Yeager, C. L. *et al*. Human aminopeptidase N is a receptor for human coronavirus 229E. *Nature*. **357**, 420–422, doi:10.1038/357420a0 (1992).
66. Delmas, B., Gelfi, J., L'Haridon, R., Sjöström, H. & Laude, H. Aminopeptidase N is a major receptor for the enteropathogenic coronavirus TGEV. *Nature.* **357**, 417–420, doi:10.1038/357417a0 (1992).
67. Usami, Y. *et al*. A 28-kDa protein with disintegrin-like structure (jararhagin-C) purified from Bothrops jararaca venom inhibits collagen-and ADP-induced platelet aggregation. *Biochem Biophys Res Commun* **201**, 331–339 (1994).
68. Siigur, J. *et al*. *Vipera lebetina* venom contains all types of snake venom metalloproteases. *Pathophysiol Haemost Thromb* **34**, 209–214 (2006).
69. Qian, J., Guo, Zy & Chi, Cw Cloning and isolation of a conus cysteine-rich protein homologous to Tex31 but without proteolytic activity. *Acta Biochim Biophys Sin (Shanghai)* **40**, 174–181 (2008).
70. Leonardi, A. *et al*. Conus consors snail venom proteomics proposes functions, pathways, and novel families involved in its venomic system. *J Proteome Res* **11**, 5046–5058 (2012).
71. Li, R. *et al*. Proteome and phosphoproteome analysis of honeybee (*Apis mellifera*) venom collected from electrical stimulation and manual extraction of the venom gland. *BMC Genomics* **14**, 1 (2013).
72. von Reumont, B. M. *et al*. The first venomous crustacean revealed by transcriptomics and functional morphology: remipede venom glands express a unique toxin cocktail dominated by enzymes and a neurotoxin. *Mol Biol Evol* **31**, 48–58 (2014).
73. Lukatela, G. *et al*. Crystal structure of human arylsulfatase A: the aldehyde function and the metal ion at the active site suggest a novel mechanism for sulfate ester hydrolysis. *Biochem* **37**, 3654–3664 (1998).
74. Buddecke, E. & Kresse, H. in *Connective Tissues*. 131–145 (Springer, 1974).
75. Shimony, T. & Nigrelli, R. Studies on arylsulphatases in the barnacle *Balanus eburneus*. *Mar Biol.* **14**, 349–358 (1972).
76. Laffy, P. W., Benkendorff, K. & Abbott, C. A. Suppressive subtractive hybridisation transcriptomics provides a novel insight into the functional role of the hypobranchial gland in a marine mollusc. *Comp Biochem Physiol Part D Genomics Proteomics* **8**, 111–122 (2013).
77. Cooksey, C. J. Tyrian purple: 6, 6′-dibromoindigo and related compounds. *Molecules.* **6**, 736–769 (2001).
78. Westley, C. B., Vine, K. L. & Benkendorff, K. In *Indirubin, the* Red Shade *of Indigo* (ed Guyard, N., Meijer, L., Skaltsounis, L. & Eisenbrand, G.) 31–44 (2006).

79. Dhevendaran, K., Kannupandi, T. & Natarajan, R. Arylsulfatase activity in marine gastropods. *Mahasagar* **13**, 173–178 (1980).
80. Spaulding, D. & Morse, D. Purification and characterization of sulfatases from Haliotis rufescens: evidence for changes in synthesis and heterogeneity during development. *J Comp Physiol B* **161**, 498–515 (1991).
81. Pesentseva, M. *et al*. A new arylsulfatase from the marine mollusk *Turbo chrysostomus*. *Chem Nat Comp* **48**, 853–859 (2012).
82. Fry, B. G. *et al*. The toxicogenomic multiverse: convergent recruitment of proteins into animal venoms. *Annu Rev Genomics Hum Genet* **10**, 483–511 (2009).
83. Yamazaki, Y. & Morita, T. Structure and function of snake venom cysteine-rich secretory proteins. *Toxicon.* **44**, 227–231 (2004).
84. Wang, J. *et al*. Blocking effect and crystal structure of natrin toxin, a cysteine-rich secretory protein from Naja atra venom that targets the BKCa channel. *Biochemistry.* **44**, 10145–10152 (2005).
85. Gibbs, G. M. *et al*. The cysteine-rich secretory protein domain of Tpx-1 is related to ion channel toxins and regulates ryanodine receptor Ca^{2+} signaling. *J Biol Chem* **281**, 4156–4163 (2006).
86. Cohen, D. J. *et al*. Cysteine-rich secretory proteins (CRISP) and their role in mammalian fertilization. *Biol Res.* **44**, 135–138 (2011).
87. Guo, M. *et al*. Crystal structure of the cysteine-rich secretory protein stecrisp reveals that the cysteine-rich domain has a K+ channel inhibitor-like fold. *J Biol Chem* **280**, 12405–12412 (2005).
88. Krätzschmar, J. *et al*. The human Cysteine-Rich Secretory Protein (CRISP) family. *Eur J Biochem* **236**, 827–836 (1996).
89. Gibbs, H. L., Sanz, L. & Calvete, J. J. Snake population venomics: proteomics-based analyses of individual variation reveals significant gene regulation effects on venom protein expression in Sistrurus rattlesnakes. *J Mol Evol* **68**, 113–125 (2009).
90. Gibbs, G. M., Roelants, K. & O'Bryan, M. K. The CAP superfamily: cysteine-rich secretory proteins, antigen 5, and pathogenesis-related 1 proteins—roles in reproduction, cancer, and immune defense. *Endocr Rev.* **29**, 865–897 (2008).
91. Yamazaki, Y., Brown, R. L. & Morita, T. Purification and cloning of toxins from elapid venoms that target cyclic nucleotide-gated ion channels. *Biochemistry.* **41**, 11331–11337 (2002).
92. Yamazaki, Y., Hyodo, F. & Morita, T. Wide distribution of cysteine-rich secretory proteins in snake venoms: isolation and cloning of novel snake venom cysteine-rich secretory proteins. *Arch Biochem Biophys* **412**, 133–141 (2003).
93. de F Fernandes-Pedrosa, M. *et al*. Transcriptome analysis of *Loxosceles laeta* (Araneae, Sicariidae) spider venomous gland using expressed sequence tags. *BMC Genomics.* **9**, 1 (2008).
94. Jiang, L. *et al*. Venomics of the spider Ornithoctonus huwena based on transcriptomic versus proteomic analysis. *Comp Biochem Physiol Part D Genomics Proteomics.* **5**, 81–88 (2010).
95. Ruiming, Z. *et al*. Comparative venom gland transcriptome analysis of the scorpion *Lychas mucronatus* reveals intraspecific toxic gene diversity and new venomous components. *BMC Genomics* **11**, 1 (2010).
96. Whittington, C. M. *et al*. Novel venom gene discovery in the platypus. *Genome Biol.* **11**, 1 (2010).
97. Morgenstern, D. *et al*. The tale of a resting gland: transcriptome of a replete venom gland from the scorpion *Hottentotta judaicus*. *Toxicon* **57**, 695–703 (2011).
98. Undheim, E. A. & King, G. F. On the venom system of centipedes (Chilopoda), a neglected group of venomous animals. *Toxicon.* **57**, 512–524 (2011).
99. Bjarnason, J. B. & Fox, J. W. Hemorrhagic metalloproteinases from snake venoms. *Pharmacol Therap* **62**, 325–372 (1994).
100. Vincent, B. *et al*. The venom composition of the parasitic wasp *Chelonus inanitus* resolved by combined expressed sequence tags analysis and proteomic approach. *BMC Genomics.* **11**, 1 (2010).
101. Shiomi, K., Kawashima, Y., Mizukami, M. & Nagashima, Y. Properties of proteinaceous toxins in the salivary gland of the marine gastropod (*Monoplex echo*). *Toxicon.* **40**, 563–571 (2002).
102. Gunji, K., Ishizaki, S. & Shiomi, K. Cloning of complementary and genomic DNAs encoding echotoxins, proteinaceous toxins from the salivary gland of marine gastropod *Monoplex echo*. *Protein J.* **29**, 487–492 (2010).
103. Terrat, Y. *et al*. High-resolution picture of a venom gland transcriptome: case study with the marine snail Conus consors. *Toxicon* **59**, 34–46 (2012).
104. Safavi-Hemami, H. *et al*. Combined proteomic and transcriptomic interrogation of the venom gland of *Conus geographus* uncovers novel components and functional compartmentalization. *Mol Cell Proteomics* **13**, 938–953 (2014).
105. Anderluh, G. & Maček, P. Cytolytic peptide and protein toxins from sea anemones (Anthozoa: Actiniaria). *Toxicon.* **40**, 111–124 (2002).
106. Ozawa, T., Kaneko, J., Nariya, H., Izaki, K. & Kamio, Y. Inactivation of γ-hemolysin H γ II component by addition of monosialoganglioside GM1 to human erythrocyte. *Biosci Biotechnol Biochem* **58**, 602–605 (1994).
107. Bellomio, A. *et al*. Purification, cloning and characterization of fragaceatoxin C, a novel actinoporin from the sea anemone *Actinia fragacea*. *Toxicon.* **54**, 869–880 (2009).
108. Dal Peraro, M. & Van Der Goot, F. G. Pore-forming toxins: ancient, but never really out of fashion. *Nat Rev Microbiol.* **14**, 77–92 (2016).
109. Mancheño, J. M., Martín-Benito, J., Martínez-Ripoll, Mn, Gavilanes, J. G. & Hermoso, J. A. Crystal and electron microscopy structures of sticholysin II actinoporin reveal insights into the mechanism of membrane pore formation. *Structure* **11**, 1319–1328 (2003).
110. Athanasiadis, A., Anderluh, G., Maček, P. & Turk, D. Crystal structure of the soluble form of equinatoxin II, a pore-forming toxin from the sea anemone *Actinia equina*. *Structure.* **9**, 341–346 (2001).
111. Malovrh, P. *et al*. A novel mechanism of pore formation membrane penetration by the N-terminal aphipathic region of equinatoxin. *J Biol Chem* **278**, 22678–22685 (2003).
112. García-Ortega, L. *et al*. The behavior of sea anemone actinoporins at the water–membrane interface. *Biochim Biophys Acta* **1808**, 2275–2288 (2011).
113. Thompson, T. Acidic allomones in marine organisms. *J Mar Biol Assoc UK* **68**, 499–517 (1988).
114. Riedel, F. An outline of cassoidean phylogeny (Mollusca, Gastropoda). *Mededelingen van de Werkgroep voor Tertiaire en Kwartaire Geologie* **32**, 97–132 (1995).
115. Wägele, H. & Klussmann-Kolb, A. Opisthobranchia (Mollusca, Gastropoda)–more than just slimy slugs. Shell reduction and its implications on defence and foraging. *Front Zool.* **2**, 1 (2005).
116. Thompson, T. Detection of epithelial acid secretions in marine molluscs: Review of techniques, and new analytical methods. *Comp Biochem Physiol Part A: Physiol* **74**, 615–621 (1983).
117. Thompson, T. Investigation of the acidic allomone of the gastropod mollusc *Philine aperta* by means of ion chromatography and histochemical localisation of sulphate and chloride ions. *J Molluscan Stud* **52**, 38–44 (1986).
118. Corner, E., Leon, Y. & Bulbrook, R. Steroid sulphatase, arylsulphatase and β-glucuronidase in marine invertebrates. *J Mar Biol Assoc UK* **39**, 51–61 (1960).

Acknowledgements

This work was supported by grants from the Australian federal government Department of the Environment Reef Rescue 'Caring for Country' program (MRH, SFC, Project ID A0000010389G). This research was undertaken with the assistance of resources provided from the Marine Research Center at Kavieng, PNG, and the NCI National Facility systems at the Australian National University through the National Computational Merit

Allocation Scheme supported by the Australian Government. We thank Varvara Barkalova for her advice on *C. tritonis* anatomy. Further thanks go to Peter Thomas-Hall for assistance in the husbandry of giant triton held at the AIMS SeaSim precinct and for filming giant tritons attacking COTS.

Author Contributions

Conceived and designed the experiment: S.F.C., C.A.M. and M.R.H. Conducted the analysis: U.B., T.W. and M.Z. Analyzed the data: U.B., T.W., C.A.M., and Z.M. Contributed reagents/materials/analysis tools: S.F.C., M.R.H. Wrote the paper: U.B., S.F.C., T.W., C.A.M. and M.R.H. Critically reviewed the manuscript: Z.M., C.A.M., M.R.H. and S.F.C.

Additional Information

Supplementary information accompanies this paper at doi:10.1038/s41598-017-05974-x

Competing Interests: The authors declare that they have no competing interests.

Publisher's note: Springer Nature remains neutral with regard to jurisdictional claims in published maps and institutional affiliations.